Journal of Particle Science and Technology *11* (2) (2025) 101-116

Iranian Research Organization for Science and Technology (IROST)

Journal of PARTICLE Science & Technology

JPSIT
https://jpst.irost.ir
Online ISSN: 2423-4079
Print ISSN: 2423-4087

Adsorption of methylene blue on lithium titanate and its composite with carbon dots: Optimization of parameters and adsorbent recovery

Mohadeseh Bazzi, Zahra Yavari✉, Mehdi Shahbakhsh

Department of Chemistry, University of Sistan and Baluchestan, Zahedan, Iran

HIGHLIGHTS

- Fabrication and characterization of porous Li_2TiO_3 (pLT)
- Incorporation of carbon dots on Li_2TiO_3 (pLT-CD)
- Analysis of the adsorption of methylene blue on pLT and pLT-CD
- Optimization of adsorption parameters

GRAPHICAL ABSTRACT

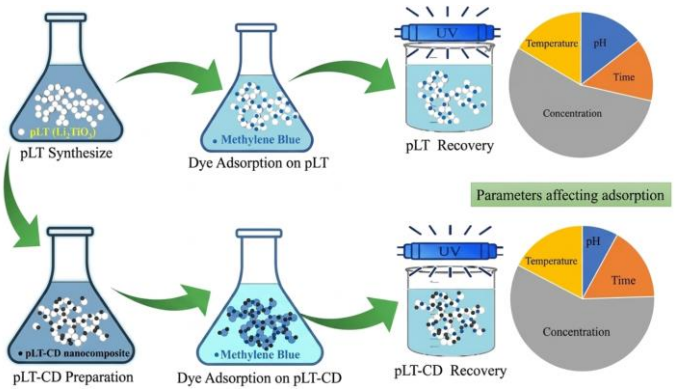

ARTICLE INFO

Article type:

Research article

Article history:

Received 09 December 2025
Received in revised form 30 March 2026
Accepted 31 March 2026

Keywords:

Taguchi method
Adsorbent recovery
Carbon dots
Porous lithium-titanium oxide
Dye removal

DOI: 10.22104/jpst.2026.8046.1288

ABSTRACT

Porous lithium-titanium oxide (pLT) was produced by the combustion synthesis method. Based on the XRD pattern, the as-synthesized powder phase was Li_2TiO_3. The carbon dots were incorporated onto the lithium titanate sponge (pLT-CD) using the microwave method and natural precursors. Two synthesized structures were used to remove methylene blue from wastewater. A morphological comparison of pLT and pLT-CD was performed using field emission scanning electron microscopy. Elemental mapping of the pLT-CD composite was used to investigate the dispersion of CD on pLT and its stability in aqueous media. The experiments of methylene blue removal by adsorbents were designed using the Taguchi method. The effect of pH, time, temperature, and methylene blue concentration on the treatment process by pLT and pLT-CD was studied. The maximum removal percentage was observed at pH 8, room temperature, 10 min, and 40 ppm dye concentration on the pLT-CD composite adsorbent. The adsorption equilibrium was better described by the Freundlich isotherm, indicating multilayer adsorption on heterogeneous surfaces. Kinetic results followed a pseudo-second-order model, with pLT-CD showing a higher adsorption rate due to enhanced surface interactions and increased active sites. Adsorbent recovery was performed by UV-Vis irradiation on the saturated adsorbent to decompose the adsorbed dye. An efficiency drop of about 20 and 13.60 % was observed for pLT and pLT-CD, respectively, after four consecutive cycles.

✉ *Corresponding author: E-mail address:* z_yavari@chem.usb.ac.ir ; *Tel:* +98-9151403565

1. Introduction

Water resources play a vital role in the lives of humans, animals, and plants. Nutrients and energy can be transported by water. Discharging industrial wastewater into water without proper treatment endangers water safety and the environment. One of the most polluting industries is the paint industry, where a significant amount of coloring compounds enter waterways through the wastewater from this industry [1].

Dye compounds have an aromatic organic structure and can absorb light and produce color in the visible range [2]. Methylene blue, with the molecular formula $C_{16}H_{18}N_3ClS$ and an aromatic heterocyclic structure [3], is an alkaline, cationic, and water-soluble molecule [4] widely consumed in the textile industry [5]. High concentrations of methylene blue in water can cause problems. The presence of methylene blue in water reduces sunlight penetration and the solubility of oxygen in the water [6]. Accumulation of this substance in mammalian organs causes cyanosis, tissue necrosis, vomiting, jaundice, shock, and increased heart rate [7]. The side effects will occur when the level of this substance in the body exceeds 7 $mg.kg^{-1}$ [8]. Therefore, it is essential to treat wastewater contaminated with methylene blue before it enters the environment. The thermal stability and non-biodegradability of this substance make it difficult to remove [9].

Some conventional techniques for methylene blue removal include: adsorption [10], phytoremediation [11,12], coagulation [13,14], biodegradation [15], photocatalytic digestion [16,17], and advanced oxidation [18]. Most of these techniques are designed to use additional chemicals or expend a lot of energy during treatment to prevent creating harmful byproducts in the water. Adsorption is a widely applied procedure for the treatment of wastewater in industries because of its high efficacy and simplicity. This process is a selective mass transfer from the wastewater mass to a solid surface. Although conventional adsorbents such as silica [19], alumina [20], carbon active [21], and biochar [22] are widely used, research is still ongoing on synthetic adsorbents such as zeolites [23], metal organic frameworks [24], ion exchange resins [25], and nanostructures [26,27] because each adsorbent has specific properties and limitations depending on its structure and composition. Some of the main reasons for continuing research on synthetic adsorbents are: selectivity, controlled surface area and porosity, chemical and thermal stability, recyclability, reusability, and multi-functionality [28-30].

Carbon structures are the dominant choice of adsorbent due to their high surface energy [31]. Carbon dots, one such structure, are zero-dimensional nanomaterials with high surface area; they are composed of small graphene sheets. In these structures, the carbon atoms are connected by sp^2 and sp^3 hybridization [32]. Studies show that functional groups containing oxygen and nitrogen are distributed on carbon dots, which improve the hydrophilicity of these structures [33]. However, the production and durability of carbon adsorbents require high costs and energy consumption. Numerous studies have been conducted on the use of cheap and readily available agricultural harvests to produce carbon adsorbents [34-36]. Using supports is one way to increase the stability of carbon adsorbents. Porous structures in the microporous (porosities < 2 nm), mesoporous (2 nm < porosities < 50 nm), and macroporous (porosities > 50 nm) range are applied for filtration, separation, and catalysis [37].

Oxide supports can be used in heterogeneous processes to stabilize and disperse carbon adsorbents and increase their performance and stability. Oxides affect the geometry of the interface between two phases in contact. Baur *et al.* developed adsorbents of activated carbon fibers combined with metal oxides for the removal of acetaldehyde from gas streams [38]. Meanwhile, the adsorbents have a macroscopic and regular structure with low resistance to fluid flow, allowing for rapid adsorption without any diffusion resistance. Therefore, it is interesting to study the synergistic effect of carbon adsorbent and oxide support in removing pollutants. A two-component absorbent of carbon nanotube-iron oxide was fabricated and used to eliminate lead (II) and copper (II) from the aquatic environment by Peng *et al.* [39]. The results of their study showed that the chemical oxidation of the adsorbent with nitric acid and the subsequent creation of functional groups on carbon nanotubes improved the removal percentage of heavy metals.

Porous oxides can show acceptable performance as adsorbents for removing pollutants from fluids due to their numerous active sites, excellent thermal and chemical stability, and non-toxicity; for example, the elimination of Congo Red by MgO with 198 $m^2.g^{-1}$ surface area [40], methylene blue by Zn-doped CeO_2 [41], and Methyl Orange by ZnO/CuO nanocomposite [42].

Despite extensive studies on dye adsorption, there remains a need for cost-effective and environmentally friendly adsorbents with improved efficiency. In this study, pLT and a novel pLT-CD composite were synthesized and characterized, where the incorporation of green-derived carbon dots enhances adsorption through increased active sites and π–π and hydrogen bonding interactions. The adsorption of methylene blue was optimized using the Taguchi method, and the process was further evaluated through kinetic and isotherm analyses. In addition, the reusability of the adsorbents and a systematic comparison

between pLT and pLT-CD were investigated to clarify the role of carbon dots in improving adsorption performance.

2. Materials and methods

2.1. Materials

All solutions used in this research work were prepared with distilled water. Sodium chloride (NaCl, Merck), tetra-butyl titanate ($Ti(OC_4H_9)_4$, Merck), nitric acid (HNO_3, Merck), lithium nitrate ($LiNO_3$, Sigma-Aldrich), and citric acid ($C_6H_8O_7$, Merck) were used in this work. Lemon and onion juices, along with 32.7 % ammonia (NH_3, Merck) solution, were employed as the main precursors in the fabrication of carbon dots. Methylene Blue dye in the form of the salt, $C_{16}H_{18}ClN_3S$. $2H_2O$ was used to produce synthetic effluent. Also, caustic soda (NaOH, Merck) and 37 % hydrochloric acid (HCl, Merck) were used in the dye removal experiments. In the present study, no further purification was performed on the commercial materials.

2.2. Instrumentation

The morphology of the two adsorbents was observed using a field-emission scanning electron microscope (FE-SEM), using a Philips XL30 instrument equipped with an SMAX energy-dispersive X-ray spectrometer. Molecular characterization was conducted using Fourier-transform infrared spectroscopy (FT-IR, Bruker Tensor II). The surface area was measured with Brunauer-Emmett-Teller (BET) theory using N_2 adsorption at 77 K via surface area analysis with a BELSORP-mini II instrument. A UV–visible spectrophotometer (V-570, Jasco, Japan) was used. A HANNA Model 213 Microprocessor pH meter was employed to adjust the pH of aquatic environments. A Sigma 101 centrifuge with a 4 cm radius was used to separate the adsorbent from the environment. The methylene blue concentration in the solution was determined with a UV-160 spectrophotometer manufactured by Shimadzu, Japan. A 900 W LG microwave was used to synthesize carbon dots. An X-ray diffraction (XRD) analyzer, Bruker Advance D8 model, Cu *Kα* radiation, and a graphite monochromator with a wavelength of 0.15406 nm were used to determine the lithium titanate phase.

2.3. Synthesis of lithium titanate

The solution combustion method was selected for the synthesis of porous lithium titanate (pLT) powders. First, 20 mmol of tetrabutyl titanate ($Ti(OC_4H_9)_4$) was combined with 75 mL of distilled water to form a pellet-shaped precipitate. Then, the precipitate was rinsed and dissolved in concentrated nitric acid (HNO_3) to fabricate a $TiO(NO_3)_2$ solution. Next, 40 mmol $LiNO_3$ and 16.66 mmol citric acid were incorporated into the as-prepared solution, and 40 mmol NaCl was introduced into the container. The mixture was stirred at room temperature to evaporate the solvent and prepare a gel-like substance. The obtained gel was heated to 450 °C by a heater stirrer until the combustion reaction occurred. Lastly, the obtained product was rinsed and dried.

2.4. Carbon dot (CD) incorporation on pLT

Carbon dots were synthesized from agricultural and horticultural wastes. Fresh lemons and onions, harvested in the autumn from the Baluchistan region of Iran, were used as natural carbon precursors. The juices were freshly extracted and used under controlled synthesis conditions to minimize compositional variability. Sedimentation and filtration were used to remove pulp pieces. Lemon juice is rich in citric acid at 6 % w/w and ascorbic acid at 64 % w/w. Both acids are suitable precursors for carbon dots. Onion juice, an essential source of sulfur compounds and ammonium hydroxide, was employed to introduce small amounts of nitrogen and sulfur heteroatoms to the carbon surface to increase the hydrophilicity of the composite surface and make it easier to use in aqueous environments in subsequent steps. Briefly, 2 ml of onion juice and 2 ml of lemon juice were combined in a 250 ml Erlenmeyer flask. Then, 10 ml of 25 % v/v ammonium hydroxide solution was prepared from a mixture of ammonia and 0.1 M sodium hydroxide. The prepared ammonium hydroxide was added to the contents of the Erlenmeyer flask along with 8 ml of double-distilled water. Next, 5 mg of the lithium titanate was dispersed into this mixture, and the mixing container was placed in a microwave at 900 W power for 7 min. After the container cooled, 100 ml of distilled water was added, allowing the precipitate to be transferred to the centrifuge tube. The precipitate was washed three times with double-distilled water by centrifugation at 3000 rpm, corresponding to an RCF of 403. Lastly, the obtained lithium titanate-carbon dot composite, hereinafter abbreviated as pLT-CD, was used as an adsorbent in subsequent studies.

2.5. Batch adsorption experiments

Methylene blue removal experiments using adsorbents were designed using the Taguchi method and Minitab17 software. An L16 orthogonal array table was set up with four factors (pH, temperature (*T*), time (*t*), and initial

concentration of methylene blue (C_0)), each with four change levels. The L16 array for four factors at four levels was selected because the number of trials was reduced from 256 (4^4) to only 16, while the distribution of levels for each factor was maintained. This reduction enabled significant savings in time and resources without compromising the statistical analysis or the evaluation of factor effects [43].

The pH of the samples was adjusted between 4 and 10 with dilute NaOH and HCl solutions. Protonation and deprotonation of the adsorbent surface are influenced by varying pH, thereby affecting its surface charge. Hence, interactions between the adsorbent and adsorbed methylene blue are affected.

Adsorption kinetics are indicated by the experiment time. The equilibrium between the two phases can be shifted by changing the operation temperature.

The tests were run at variable times of 10 to 40 min and temperatures of 20 to 50 °C. The initial concentration was considered a key factor in dye adsorption, as it determines the ratio of dye molecules to available adsorption sites. Levels of 10, 20, 30, and 40 ppm were chosen to evaluate the effects of adsorbent saturation and concentration on removal efficiency.

The concentration of dye adsorbed on the adsorbent is determined by two factors: the concentration of dye in the media and the mass density of active sites on the adsorbent. The density of active sites of the two structures is compared by varying the initial concentration of dye (C_0) between 10 and 40 ppm in the solution.

The adsorbent mass was 0.008 g in all batch experiments. The solution agitation was provided by a magnetic stirrer at about 100 rpm. After the end of each test run, the adsorbent was separated by sedimentation and centrifugation. The absorbance of the filtered solution was determined by the spectrophotometer at 665 nm wavelength, where maximum absorption occurs for methylene blue. The concentration of the remaining methylene blue in the solution was measured using a calibration plot.

The batch experiments were conducted under dark conditions to ensure that only the adsorption process (and no photocatalytic degradation) contributed to dye removal.

2.6. Absorbents recovery method

As mentioned in the introduction, one of the methods for treating colored wastewater is its photocatalytic digestion. In this technique, the oxidation of colored pollutants is carried out under ultraviolet light irradiation and in the presence of a photocatalytic semiconductor. This method is limited by large quantities of wastewater, which reduces the penetration of ultraviolet light. Hence, there is a need to build shallow ponds. Time-consuming and limited efficiency are the main challenges of this technique. In the present work, photocatalytic digestion has been used to recover dye-saturated adsorbents. In order to recover the dye-saturated adsorbents, the collected powder was dispersed in water (0.5 $g.L^{-1}$) and exposed to UV light at a wavelength of 254 nm at three time intervals. It is known that the band gap of carbon dots is in the range of 2.8 to 4 eV [44]. The indirect band gap energy of pLT has been found to be 3.92 eV [45]. Oxidation of the adsorbed dye and its removal is facilitated by the photocatalytic behavior of the two components. To evaluate the performance of the adsorbent after recovery, the percentage of dye elimination was calculated at pH 8, temperature 30 °C, initial concentration 40 ppm for methylene blue, and contact time 10 min during four steps (each step after recovery of the adsorbent).

3. Results and discussion

3.1. Adsorbents characterization

Initially, the structural phase, particle size, and morphology of the synthesized lithium titanium oxide sample were identified. The X-ray diffraction (XRD) pattern for the lithium titanate powder is shown in Fig. 1. The pattern provided is found to correspond to card number 0831-033. Thus, Li_2TiO_3 was identified as the phase of the synthesized powder. A crystallite size of approximately 30 nm was estimated for the synthesized powder.

The FT-IR spectrum of the pLT-CD sample is shown in Fig. 1(b). The characteristic broad absorption peak at 3256 cm^{-1} was assigned to hydrogen-bonded species such as N–H and O–H [46]. The bands at 1624 and 1033 cm^{-1} were associated with double bonds of carbons and single bonds of carbons with heteroatoms, respectively [47]. The bands at 469 and 633 cm^{-1} were characteristic vibrations of the Ti–O bond, indicating the formation of lithium titanate [48].

The surface area of pLT and pLT-CD powders was estimated using BET analysis as 50.21 and 54.62 $m^2.g^{-1}$, respectively. The as-prepared absorbent caused the high surface area.

The absorption spectrum of CD (Fig. 1(c)) showed two significant bands, which were located at 212 nm, assigned to the π–π* transition of C=C and C–C bonds in the sp^2 hybridized domain of the graphitic core, and at 280 nm, attributed to the n–π* transition of C=O [49].

To better investigate the size and morphology of the two adsorbents, FE-SEM analysis was performed on pLT and pLT-CD samples. Fig. 2 illustrates FE-SEM micrographs of the synthesized samples at a scale of 200 nm. In Fig. 2(a), the

particles with a spherical shape and uniform morphology are visible in the image. The particle size was between 30 and 40 nm, and the dimensions of the inter-particle pores were 20 to 30 nm, proving that the synthesized lithium titanate was a nanoscale and mesoporous powder.

During the solution combustion synthesis to produce pLT, upon heating of the reaction mixture, evaporation of the solvent and release of CO_2, CO, H_2O, and N_2 gases were induced; as a result, the product was synthesized in a porous form. Fig. 2(b) presents the FE-SEM image of the pLT-CD. An acceptable distribution of carbon dots on the surface and within the pores of lithium titanate is indicated by the uniform morphology of the composite. The suitability of the two introduced structures for heterogeneous adsorption of methylene blue is indicated by the observed porosity in Figs. 2(a) and 2(b).

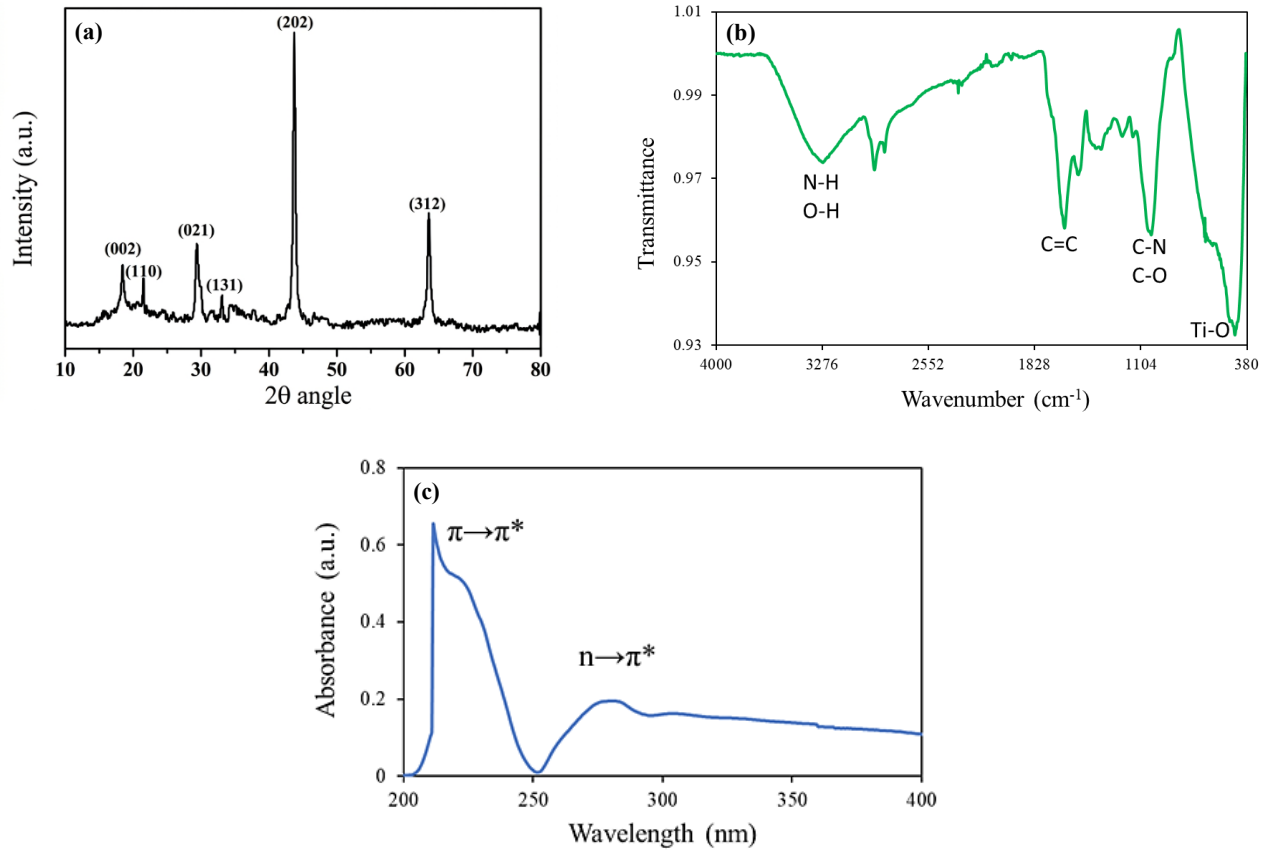

Fig. 1. (a) XRD Pattern of pLT, (b) FT-IR spectrum of pLT-CD, and (c) UV spectrum of CD sample.

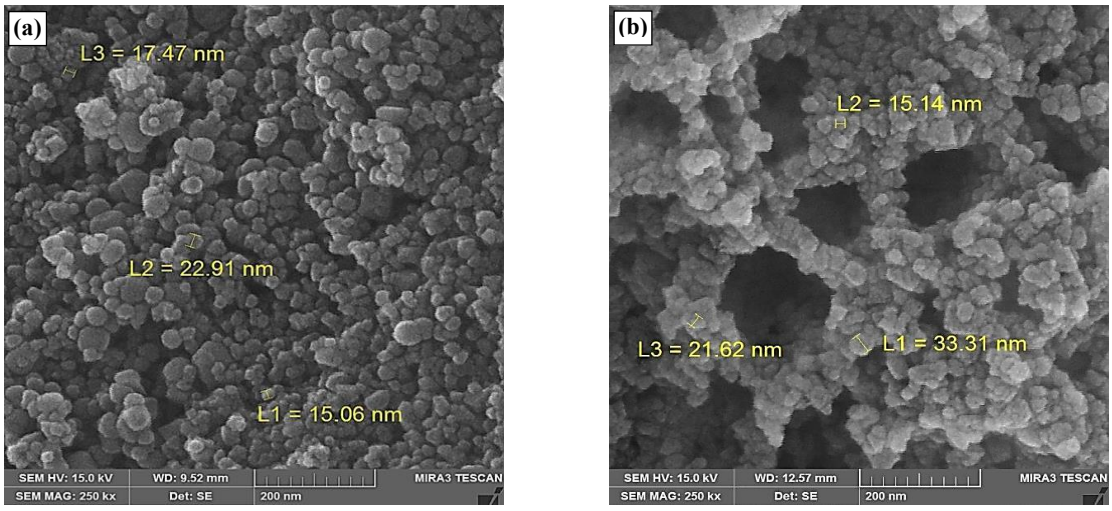

Fig. 2. FE-SEM Micrographs of (a) lithium titanate and (b) lithium titanate-carbon dot composite at a magnification of 250,000× (scale bar: 200 nm).

High dispersion of carbon dots in water due to surface carboxyl groups is considered a major challenge that can compromise the stability of the adsorbent. The pLT-CD sample was immersed in water for 4 h to study the effectiveness of using pLT support for CDs to prevent their entry into water. After separating the composite particles from the water, elemental mapping analysis was performed to investigate the presence and dispersion of carbon.

The results are represented in Fig. 3. It should be noted that the element lithium was not detectable due to its small atomic radius. Successful loading and stability of carbon dots on the lithium titanate surface are confirmed by the presence of carbon.

The effectiveness of the microwave method in synthesizing carbon dots on the oxide substrate is indicated by the uniform dispersion of carbon. This uniform dispersion and persistence of carbon dots on the surface could be attributed to the high porosity of the oxide substrate and the applied microwave power.It is possible that the nanoscale pores in the lithium titanate structure served as traps for carbon dots, thereby preventing their removal by the aqueous medium.

The purity of the synthetic composite is indicated by the absence of other elements.

3.2. Parameter optimization with batch experiments

Methylene blue removal experiments using adsorbents were designed using the Taguchi method, and an L16 orthogonal array table was set up with four factors (pH, temperature (T), time (t), and initial concentration of methylene blue (C_0)), each with four change levels (see Table 1). The results were calculated as the removal percentage (R %) of methylene blue, according to Eq. (1).

$$R\ \% = (C_0\text{-}C_e) \times 100 / C_0 \quad (1)$$

The methylene blue concentration before removal is denoted by C_0, and the remaining concentration after adsorption is denoted by C_e. In the experimental design, the effect of input factors is considered based on maximizing the removal percentage of methylene blue. In the Taguchi method, a transformed response function is used for accurate statistical analysis of the results. It can be defined as the ratio of the signal of each effect or effects to the error or noise.

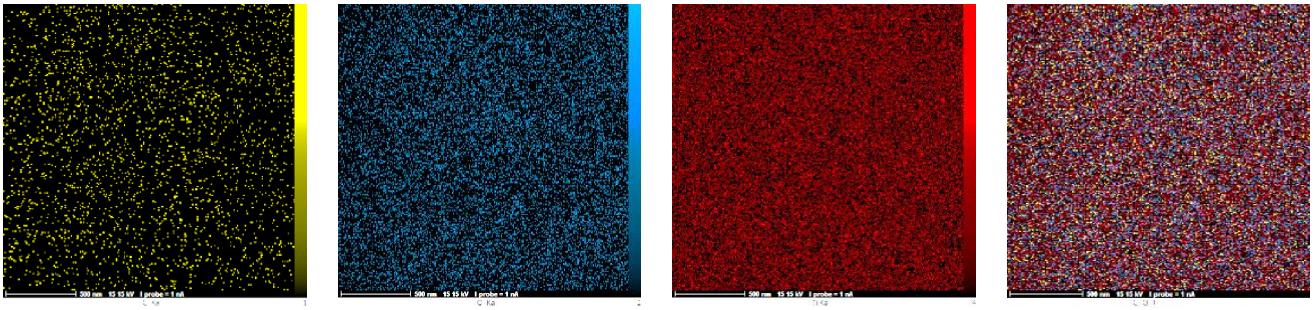

(a) **(b)** **(c)** **(d)**

Fig. 3. Elemental mapping of (a) carbon, (b) oxygen, (c) titanium, and (d) merged C-O-Ti for pLT-CD composite.

Table 1. Removal percentage for methylene blue obtained by a combination of experiments proposed by the Taguchi method.

Run order	pH	T (°C)	C_0 (ppm)	t (min)	pLT	pLT-CD
1	4	20	10	10	77.92	82.79
2	4	30	20	20	83.53	82.01
3	4	40	30	30	87.24	90.62
4	4	50	40	40	86.72	91.45
5	6	40	20	10	84.98	88.76
6	6	50	30	20	68.50	77.86
7	6	20	40	30	89.65	91.20
8	6	30	30	40	87.62	84.98
9	8	50	30	10	89.45	92.12
10	8	40	40	20	90.25	92.25
11	8	30	10	30	79.60	78.26
12	8	20	20	40	87.06	87.48
13	10	30	40	10	93.84	92.62
14	10	20	30	20	88.70	91.35
15	10	50	20	30	81.73	86.36
16	10	40	10	40	72.31	77.69

In this study, the response considered is the removal percentage. The ratio of signal to noise (S/N) is determined by Eq. (2).

$$S/N = -10\log\frac{\left(\frac{1}{y_1^2}+\frac{1}{y_2^2}+\cdots+\frac{1}{y_n^2}\right)}{n} \quad (2)$$

In this equation, the measured response value for each experiment in each test is denoted by y_n, and the number of repetitions of the experiments is denoted by n. To determine the optimal conditions for each factor, i.e., the maximum mean S/N rate of each parameter among the four levels and predict the four optimal factors based on analytical methods, the mean S/N rate of each parameter was measured at four levels, and the maximum S/N obtained was marked as the optimal level of that factor (see Fig. 4).

The adsorption phenomenon is significantly affected by the solution pH. As shown in Fig. 4(a), the optimum pH for both adsorbents is 8. At low pH, accumulation of H^+ ions occurs on the adsorbent surface, resulting in the acquisition of a positive charge by the adsorbent surface, which causes repulsion between the cationic dye methylene blue and the adsorbent surface. As the pH increases, a negative charge is acquired by the functional groups on the adsorbent surface, leading to electrostatic attraction of the adsorbent surface to the methylene blue.

With enhanced adsorption, the dye concentration in the solution is decreased, and accumulation on the adsorbent surface is increased.

Hence, the dye transfer from the solid surface to the solution is predictable. The removal percentage for the dye was investigated in the contact time range of 10 to 40 min. For methylene blue, as revealed in Fig. 4(b), adsorption occurred at a high rate during the first 10 min, after which equilibrium was reached by the system.

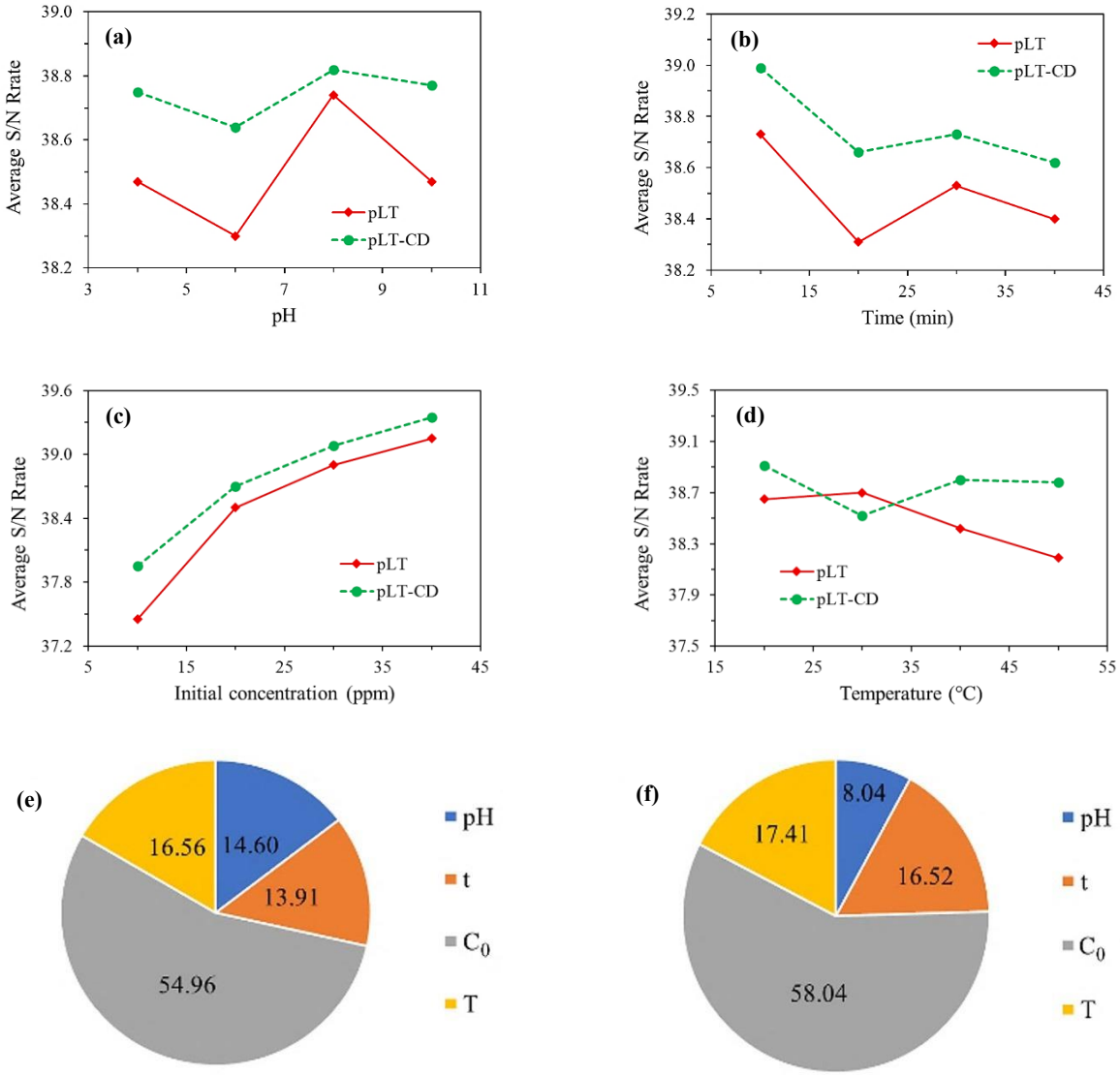

Fig. 4. Average output S/N for (a) pH, (b) time, (c) initial concentration (C_0), and (d) temperature parameters; and percentage of parameters effect on the performance of methylene blue removal by (e) pLT and (f) pLT-CD adsorbents.

The C_0 effect was investigated on the elimination of dye, and the optimum concentration was found to be 40 ppm, as shown in Fig. 4(c). Based on experience, with increasing concentration, the number of available sites is reduced, and at low concentrations, the binding sites on the adsorbent surface can be contacted by the dye in solution.

Due to the high adsorption surface area and high porosity of the adsorbent and as well as the abundance of active sites at low concentrations, an increase in concentration results in enhanced removal percentage.

Examination of the performance of the two adsorbents demonstrates that a higher efficiency is observed for pLT-CD compared to pLT (Fig. 4(c)).

This can be attributed to two factors: (i) a larger number of active sites and (ii) more diverse and stronger interactions between the dye molecule and the adsorbent for the methylene blue adsorption on pLT-CD compared to pLT. Formation of cation-π bonds is expected to occur in the pLT adsorbent due to electrostatic forces between the polarized regions caused by the cation and the quadrupole of the electron-rich aromatic structures [50]. In the pLT-CD adsorbent, easier adsorption is facilitated by π-π interactions of the dye molecule with the hexagonal cells of the CD structure, in addition to the heteroatom-containing functional groups [51]. Hydrogen bonds may be formed between the electronegative heteroatoms in CD and the methylene blue molecule in aqueous solution. The changes in trend for the two adsorbents are observed to be opposite to each other, as shown by the behavior of the plot in Fig. 4(d).

The optimal temperature was selected as room temperature, according to Figs. 4(e) and 4(f), the highest effect on the elimination of methylene blue is observed for C_0.

A more noticeable effect on the removal of dye by pLT compared to pLT-CD is exerted by the pH factor. According to the signal-to-noise plots, the highest amount of color removal by pLT adsorbent is observed at pH 8, time 10 min, temperature 30 °C, and concentration 40 ppm. The order of the most effective factors for methylene blue removal by pLT is: initial concentration > temperature > pH > time. Also, for the pLT-CD adsorbent, the maximum R % is expected at pH 8, time 10 min, concentration 40 ppm, and temperature 20 °C. The most effective factors for removal with pLT-CD adsorbent are:
initial concentration > temperature > time > pH.

According to the results, pH had a greater effect on the adsorption process of methylene blue on pLT compared to pLT-CD, meaning that the adsorption mechanism was different in these two materials. The adsorption of methylene blue (which is a cationic dye) on pLT depended on the surface charge of the adsorbent. The change in pH caused a change in the surface charge due to protonation or deprotonation of the adsorbent surface. At high pH, the negative surface charge and electrostatic attraction occurred more. In the case of the pLT-CD adsorbent, the presence of carbon dots in the composite led to a number of important events such as: (i) the creation of various functional groups, (ii) an increase in the surface area, and (iii) the creation of additional interactions such as π-π stacking, hydrogen bonding, and van der Waals. Therefore, the adsorption on this adsorbent was not limited to surface charge and electrostatic force, and several other mechanisms were also active, which did not change significantly with the change in the surface charge of the adsorbent.

The higher optimum temperature observed for pLT indicated that the adsorption process was endothermic in nature, such that increasing the temperature increased the mobility of methylene blue molecules and facilitated their diffusion to the active sites. In contrast, pLT-CD showed maximum adsorption at a lower temperature, indicating an exothermic adsorption process. The presence of carbon dots induced several strong interactions such as π-π stacking and hydrogen bonding, which were more favorable at lower temperatures and tended to weaken with increasing temperature. Therefore, the addition of carbon dots not only reduced the energy requirement for adsorption, but also changed the thermodynamic nature of the process from a predominantly endothermic to an exothermic behavior.

Based on simple linear regression analysis of experimental data, the predicted removal efficiency under optimal conditions is 91.75 % for pLT and 94.37 % for pLT-CD, indicating that a higher methylene blue removal performance is achieved by pLT-CD compared to pLT. The addition of carbon dots to the adsorbent structure results in an increase in active sites, porosity, and π–π as well as hydrogen-bonding interactions; therefore, a better and faster adsorption performance is achieved.

3.3. Efficiency comparison of recovered adsorbents

The optimization of the adsorbent recovery time under ultraviolet light irradiation was performed at times of 4, 8, and 12 h (Fig. 5(a)). As can be seen, shorter recovery times lead to reduced adsorbent efficiency. Therefore, 12 h of irradiation was chosen to recover the adsorbent for further work. The percentage of methylene blue removal (R %) was calculated at optimized conditions during four steps and each step after recovery of the adsorbent. Each test run was repeated three times, and the means were reported.

Figs. 5(b) and 5(c) show the changes in color removal efficiency for the adsorbents obtained from each recovery

step. The recovery process in the first and second stages did not have a significant effect on the adsorbent performance in dye elimination; however, a decrease in efficiency was observed for the adsorbent in the third and fourth stages. This decrease is due to surface contamination by adsorbed dye, which would continue to occupy the adsorbent surface.

It is likely that at high frequencies of use, the possibility of sintering of the adsorbent particles and the release of carbon dots from the oxide surface would reduce the surface area and make it difficult for ultraviolet radiation to decompose the dye.

As a result, the adsorbent surface will remain contaminated. The efficiency loss for pLT and pLT-CD is 20 and 13.60 %, respectively. Therefore, lithium titanate decorated with carbon dots may be a suitable option for the surface adsorption process for methylene blue dye removal.

3.4. Analysis of adsorption isotherms

The relationship between the equilibrium concentration of the adsorbate and the mass of the adsorbed substance per unit mass of adsorbent (called q_e) during a process at constant temperature is known as the adsorption isotherm. The adsorption process of methylene blue onto pLT and pLT-CD was evaluated by the Freundlich and Langmuir models via linear regression in Fig. 6. The adsorption mechanism of methylene blue on pLT and pLT-CD is elucidated by the analysis of the isotherm parameters presented in Table 2.

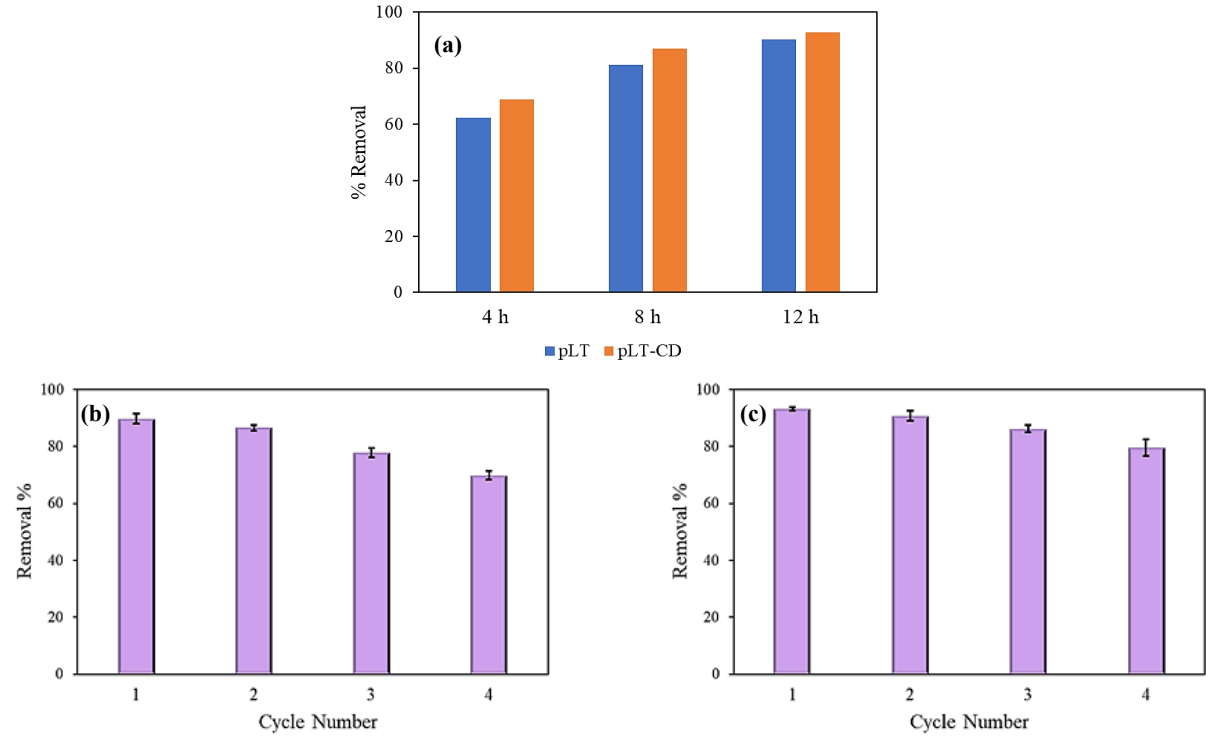

Fig. 5. Bar graph of the average percentage of methylene blue removal on the recovered adsorbent with irradiation (a) at different times, (b) pLT, and (c) pLT-CD at 12 h, with the standard deviation for three repeats at each cycle.

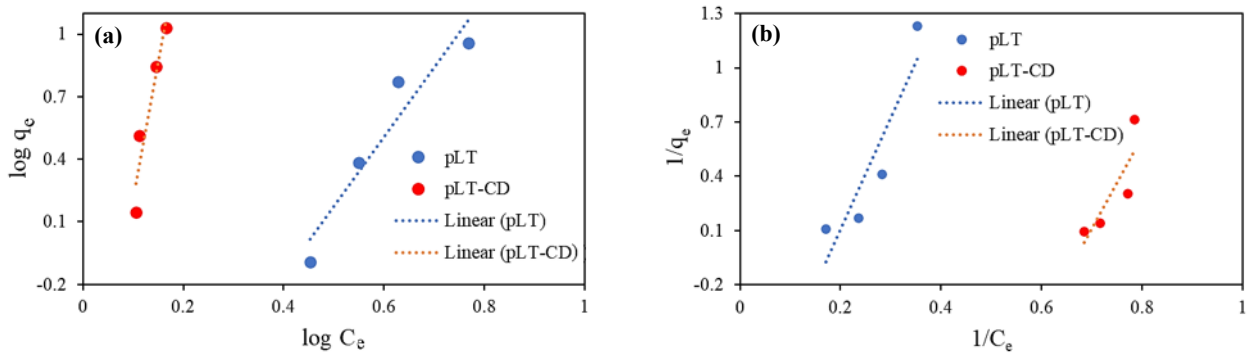

Fig. 6. Linear fit of (a) Freundlich and (b) Langmuir isotherm models of methylene blue adsorption on pLT and pLT-CD.

Table 2. Parameters of isotherm models for methylene blue adsorption.

Isotherm model	Material	*K*	*n*	R^2
Freundlich: $\log q_e = \frac{1}{n}\log C_e + \log K$	pLT	0.033	0.302	0.914
	pLT-CD	0.077	0.075	0.907
Langmuir: $\frac{1}{q_e} = \frac{1}{K\,C_e} + \frac{a}{K}$	pLT	0.163	-0.182	0.835
	pLT-CD	0.197	-0.677	0.720

Good agreement was observed between the Freundlich model and the equilibrium adsorption data of methylene blue. Well-defined straight lines with high linear regression coefficients were obtained for the two tested adsorbents using the linear model. On the other hand, a correct description of the adsorption process was not provided by the Langmuir model, as regression coefficients far from unity and unrealistic negative adsorption energy (labeled a in Table 2) values were obtained. It is suggested that the adsorption occurs mainly on energetically heterogeneous surfaces rather than through an ideal monolayer coating. Furthermore, favorable adsorption with surface heterogeneity and possible cooperative interactions is indicated by the Freundlich exponent ($n < 1$). Numerous adsorption sites with different surface energies are provided by the porous structure of lithium titanate, while Electrostatic adsorption toward cationic methylene blue molecules is promoted by surface oxygen atoms (Ti–O, surface hydroxyl groups). Surface heterogeneity is further enhanced and adsorption affinity is increased by the addition of carbon dots through the introduction of oxygen-containing functional groups and π-conjugated domains. It is confirmed by the deviation from the Langmuir model and the emergence of unrealistic constants that the adsorption does not follow a uniform monolayer mechanism but proceeds through multilayer formation on a heterogeneous porous surface, mainly controlled by electrostatic attraction and π-π interactions. As a result, multilayer adsorption with non-uniform distribution of heat and affinity over the heterogeneous surface was observed for methylene blue on both adsorbents based on the Freundlich isotherm [52]. The physical nature of the adsorption process is indicated by the better fit of the data to the Freundlich isotherm than the Langmuir isotherm, particularly at low temperatures [53].

3.5. Kinetics of adsorption

Batch experiments were performed under optimal conditions with different times to evaluate the adsorption kinetics of methylene blue onto pLT and pLT-CD; and the experimental data were fitted linearly with two models (See Table 3). It is known that the adsorption capacity is affected by many factors, and the influence of observable parameters on the overall rate of the process is only accounted for by a typical kinetic model [54].

The adsorption rate is described by the pseudo-first-order model, and is considered to depend on the available sites in the adsorbent for the physical adsorption process, whereas the adsorption reaction rate is described by the pseudo-second-order model with energetically heterogeneous sites dependent on the adsorbent, and is considered a chemisorption model [55]. According to Table 3, acceptable agreement with the pseudo-second-order kinetic model was observed for the experimental data.

The kinetic results show that the adsorption of methylene blue onto both pLT and pLT-CD follows a pseudo-second-order model with excellent fit, indicating that the adsorption rate is controlled by surface interactions and not solely by external mass transfer.

The acceleration of the adsorption process by carbon dot modification is confirmed by the higher second-order rate constant for pLT-CD (k_2 = 0.14 g.mg^{-1}.min^{-1}) compared to pLT (k_2 = 0.07 g.mg^{-1}.min^{-1}). This enhancement can be attributed to the improvement of surface reactivity, increased active sites, and stronger electronic interactions between the π-electron system of methylene blue and the graphitic domains of carbon dots. Meanwhile, the diffusion of the dye is facilitated by the porous lithium titanate matrix through its interconnected pore lattice.

Therefore, the adsorption mechanism can be described as a surface-controlled process involving heterogeneous active sites, in which the rate-limiting step is collectively controlled by electrostatic attraction, surface complex formation, and π–π interactions.

4. Conclusion

In summary, lithium titanate was prepared by solution combustion to obtain a sponge structure of pure, nanometer-sized crystalline particles. Onion and lemon juices were used to deposit carbon dots on the porous oxide surface by the microwave method. High porosity was observed in FE-SEM images of the two adsorbents (pLT and pLT-CD); therefore, the introduced structures were selected for heterogeneous adsorption processes of colored pollutants from wastewater.

Table 3. Kinetic parameters for the adsorption of methylene blue.

Model		Parameter	pLT	pLT-CD
Pseudo first-order:	$\log(q_e - q_t) = log(q_e) - \frac{K_1 t}{2{,}303}$	k_1	0.31	0.61
		q_e	8.05	8.21
		R^2	0.99	0.87
Pseudo second-order:	$\frac{t}{q_t} = \frac{1}{k_2 q_e^2} + \frac{t}{q_e}$	k_2	0.07	0.14
		q_e	14.58	14.60
		R^2	0.99	1.00

q_e: Equilibrium adsorption capacity (mg.g^{-1}); q_t: Time adsorption capacity (mg.g^{-1}); t: Time (min); k_1: First-order rate coefficient (min^{-1}); and k_2: Second-order rate coefficient (g.mg^{-1}.min^{-1}).

The loading and stabilization of carbon dots on lithium titanate were confirmed by elemental mapping. The effect of effective parameters was investigated on the adsorption of methylene blue on pLT and pLT-CD adsorbents using experimental design and the Taguchi method. The adsorption mechanism of methylene blue on pLT was mainly controlled by electrostatic interactions. Changes in pH significantly changed the surface charge of the adsorbent, while higher temperatures increased the adsorption, indicating an endothermic process. In contrast, the pLT-CD composite showed a more complex adsorption mechanism involving multiple interactions such as electrostatic attraction, π-π stacking, and hydrogen bonding. As a result, the adsorption process was less sensitive to pH and more favorable at lower temperatures, indicating an exothermic nature. The addition of carbon dots changed the adsorption mechanism from a predominantly electrostatic and temperature-dependent process to a multi-interaction system with less dependence on environmental conditions.

A higher methylene blue adsorption efficiency was observed for pLT-CD compared to pLT, which can be attributed to the combined effect of the increased specific surface area and the modification of surface chemistry induced by carbon dot incorporation. The larger surface area provides more accessible active sites, while the altered surface functional groups promote stronger and more diverse interactions with the dye molecules. The adsorption of methylene blue on the adsorbents was shown to follow the Freundlich isotherm and pseudo-second-order kinetics. Table 4 shows a comparative evaluation of available adsorbents for the removal of methylene blue dye [56-63]. The greatest effect on the elimination of methylene blue by both adsorbents was observed for the initial concentration of methylene blue.

The adsorption mechanism of methylene blue on both adsorbents was governed by heterogeneous surface interactions, with a good fit to the Freundlich model and confirmation of the deviation from ideal monolayer behavior. Furthermore, the dominance of pseudo-second-order kinetics and the increase in rate constant for pLT-CD indicated that the carbon dot modification significantly improved the adsorption performance through stronger surface interactions and accelerated adsorption rate.

The dye-saturated adsorbents were exposed to ultraviolet radiation to decompose the adsorbed dye and release it from the adsorbent surface. The recovered adsorbent was used to remove the dye again. The efficiency loss in the adsorbent with carbon dots was less than that without carbon dots.

Table 4. Comparison of methylene blue adsorption capacity under different conditions and adsorbents.

Adsorbent	Adsorption capacity (mg.g^{-1})	pH	Temperature (°C)	Contact Time (min)	Ref.
Raw beech sawdust	9.78	~6	25	120	[56]
Neem sawdust	3.62	~6	30	180	[57]
Beer brewery waste	4.92	6-7	30	60	[58]
Cow dung ash	5.31	~7	25	90	[59]
Coir pith carbon	5.87	6-7	30	60	[60]
PANI Nanotube base/silica	10.3	~7	25	120	[61]
PProDOT/MnO_2	13.94	7	25	60	[62]
CMC-*g*-poly(acrylamide)/biochar	High removal	10	25	50	[63]
pLT	13.89	10	30	60	This work
pLT-CD	14.07	10	20	60	This work

The cost and environmental compatibility of the prepared adsorbents have been of interest. pLT is synthesized from relatively readily available precursors, and although lithium-based materials may be relatively expensive, their high efficiency and reusability compensate for the initial cost. The incorporation of carbon dots from natural precursors further improves the cost-effectiveness and stability of pLT-CD. Compared with conventional adsorbents such as activated carbon, MOFs, and graphene-based materials, the prepared adsorbents offer a balanced combination of performance, lower synthesis complexity, and improved environmental compatibility. Furthermore, their low toxicity and chemical stability make them promising environmentally friendly candidates for wastewater treatment.

Funding

Financial support for this study was provided by the Research Council of the University of Sistan and Baluchestan.

Conflict of interest

The authors declare no conflicts of interest regarding this manuscript.

References

[1] Wong, S., Ghafar, N. A., Ngadi, N., Razmi, F. A., Inuwa, I. M., Mat, R., & Amin, N. A. (2020). Effective Removal of Anionic Textile Dyes Using Adsorbent Synthesized from Coffee Waste. *Scientific Reports*, *10*, 2928. https://doi.org/10.1038/s41598-020-60021-6

[2] Abd-Elhamid, A. I., Emran, M., El-Sadek, M. H., El-Shanshory, A. A., Soliman, H. M., Akl, M. A., & Rashad, M. (2020). Enhanced Removal of Cationic Dye by Eco-Friendly Activated Biochar Derived from Rice Straw. *Applied Water Science*, *10*, 45. https://doi.org/10.1007/s13201-019-1128-0

[3] Sahu, S., Pahi, S., Sahu, J. K., Sahu, U. K., & Patel, R. K. (2020). Kendu (*Diospyros Melanoxylon Roxb*) Fruit Peel Activated Carbon - An Efficient Bioadsorbent for Methylene Blue Dye: Equilibrium, Kinetic, and Thermodynamic Study. *Environmental Science and Pollution Research*, *27*, 22579-22592. https://doi.org/10.1007/s11356-020-08561-2

[4] Wei, X., Wang, Y., Feng, Y., Xie, X., Li, X., & Yang, S. (2019). Different Adsorption-Degradation Behavior of Methylene Blue and Congo red in Nanoceria/H_2O_2 System under Alkaline Conditions. *Scientific Reports*, *9*, 4964. https://doi.org/10.1038/s41598-018-36794-2

[5] Derakhshan, Z., Baghapour, M. A., Ranjbar, M., & Faramarzian, M. (2013). Adsorption of Methylene Blue Dye from Aqueous Solutions by Modified Pumice Stone: Kinetics and Equilibrium Studies. *Health Scope*, *2*(3), 136-144. https://doi.org/10.17795/jhealthscope-12492

[6] Kosswattaarachchi, A. M., & Cook, T. R. (2018). Repurposing the Industrial Dye Methylene Blue as an Active Component for Redox Flow Batteries. *ChemElectroChem*, *5*(22), 3437-3442. https://doi.org/10.1002/celc.201801097

[7] Fernando, S. M., Tran, A., Soliman, K., Flynn, B., Oommen, T., Wenzhe, L., Adhikari, N. K. J., Kanji, S., Seely, A. J. E., Fox-Robichaud, A. E., Wax, R. S., Cook, D. J., Lamontagne, F., & Rochwerg, B. (2024). Methylene Blue in Septic Shock: A Systematic Review and Meta-Analysis. *Critical Care Explorations*, *6*(7), e1110. https://doi.org/10.1097/CCE.0000000000001110

[8] Bistas, E., & Sanghavi, D. K. (2023). Methylene Blue. In *StatPearls* [Internet]. StatPearls Publishing. https://www.ncbi.nlm.nih.gov/books/NBK557593/

[9] Khan, I., Saeed, K., Zekker, I., Zhang, B., Hendi, A. H., Ahmad, A., Ahmad, S., Zada, N., Ahmad, H., Shah, L. A., Shah, T., & Khan, I. (2022). Review on Methylene Blue: Its Properties, Uses, Toxicity and Photodegradation. *Water*, *14*(2), 242. https://doi.org/10.3390/w14020242

[10] Liu, T., Li, Y., Du, Q., Sun, J., Jiao, Y., Yang, G., Wang, Z., Xia, Y., Zhang, W., Wang, K., Zhu, H. & Wu, D. (2012). Adsorption of Methylene Blue from Aqueous Solution by Graphene. *Colloids and Surfaces B: Biointerfaces*, *90*, 197-203. https://doi.org/10.1016/j.colsurfb.2011.10.019

[11] Imron, M. F., Kurniawan, S. B., Soegianto, A., & Wahyudianto, F. E. (2019). Phytoremediation of Methylene Blue Using Duckweed (*Lemna minor*). *Heliyon*, *5*(8), e02206. https://doi.org/10.1016/j.heliyon.2019.e02206

[12] Urucu, O. A., Garosi, B., & Musah, R. A. (2025). Efficient Phytoremediation of Methyl Red and Methylene Blue Dyes from Aqueous Solutions by *Juncus effusus*. *ACS Omega, 10*(2), 1943-1953. https://doi.org/10.1021/acsomega.4c07468

[13] Sugha, A., & Bhatti, M. S. (2025). Optimization of Electrocoagulation Removal of a Mixture of Three Azo Dyes: Spectrophotometric Colour Characteristics for Best Operating Conditions. *RSC Advances*, *15*(9), 6492-6505. https://doi.org/10.1039/D4RA08485C

[14] Lau, Y. Y., Wong, Y. S., Teng, T. T., Morad, N., Rafatullah, M., & Ong, S. A. (2015). Degradation of Cationic and Anionic Dyes in Coagulation–Flocculation

Process Using Bi-Functionalized Silica Hybrid with Aluminum-Ferric as Auxiliary Agent. *RSC Advances*, *5*(43), 34206-34215. https://doi.org/10.1039/C5RA01346A

[15] Cui, C., Li, D., & Wang, L. J. (2025). Biodegradable Genipin Cross-Linked Chitosan/Pea Protein Isolate Sponges for Effective Adsorption of Methyl Blue: Batch Experiments and Quantum Chemical Analysis. *Separation and Purification Technology*, *358*(part B), 130425. https://doi.org/10.1016/j.seppur.2024.130425

[16] Abdelkader, M. S., Younis, S. A., El-Fawal, E. M., Ali, H. R., & Ibrahim, H. (2025). Ag_3PO_4@ZnO Kraft Lignin Composite for Optimized Photocatalytic Degradation of Methylene Blue Using Rsponse Surface Methodology. *Scientific Reports*, *15*, 20165. https://doi.org/10.1038/s41598-025-05597-7

[17] Mahdavi, M., Mirmohammadi, M., Baghdadi, M., & Mahpishanian, S. (2022). Visible Light Photocatalytic Degradation and Pretreatment of Lignin Using Magnetic Graphitic Carbon Nitride for Enhancing Methane Production in Anaerobic Digestion. *Fuel*, *318*, 123600. https://doi.org/10.1016/j.fuel.2022.123600

[18] Hoang, N. T., Manh, T. D., Nguyen, V. T., Nga, N. T., Mwazighe, F. M., Nhi, B. D., Hoang, H. Y., Chang, S. W., Chung, W. J., & Nguyen, D. D. (2022). Kinetic Study on Methylene Blue Removal from Aqueous Solution Using UV/Chlorine Process and Its Combination with Other Advanced Oxidation Processes. *Chemosphere*, *308*(part 3), 136457. https://doi.org/10.1016/j.chemosphere.2022.136457

[19] Marey, A., Gado, W. S., Soliman, A. G., Masoud, A. M., El-Zahhar, A. A., Al-Hazmi, G. A., Taha, M. H., & El Naggar, A. M. (2024). Efficient Removal of Methylene Blue Dye from Wastewater Specimen Using Polystyrene Coated Nanoparticles of Silica. *Inorganic Chemistry Communications*, *160*, 112018. https://doi.org/10.1016/j.inoche.2024.112018

[20] Hussein, E. B., & Rasheed, F. A. (2025). Innovative Use of Recycled Aluminum Adsorbent for Methylene Blue Adsorption and Post-Application for Soil Stabilization. *Journal of Contaminant Hydrology*, *272*, 104553. https://doi.org/10.1016/j.jconhyd.2025.104553

[21] Dimbo, D., Abewaa, M., Adino, E., Mengistu, A., Takele, T., Oro, A., & Rangaraju, M. (2024). Methylene Blue Adsorption from Aqueous Solution Using Activated Carbon of *Spathodea campanulata*. *Results in Engineering*, *21*, 101910. https://doi.org/10.1016/j.rineng.2024.101910

[22] Trivedi, Y., Sharma, M., Mishra, R. K., Sharma, A., Joshi, J., Gupta, A. B., Achintya, B., Shah, K., & Vuppaladadiyamd, A. K. (2025). Biochar Potential for Pollutant Removal During Wastewater Treatment: A Comprehensive Review of Separation Mechanisms, Technological Integration, and Process Analysis. *Desalination, 600,* 118509. https://doi.org/10.1016/j.desal.2024.118509

[23] Le, T. P., Luong, H. V., Nguyen, H. N., Pham, T. K., Le, T. L., Tran, T. B., & Ngo, T. N. (2024). Insight into Adsorption-Desorption of Methylene Blue in Water Using Zeolite NaY: Kinetic, Isotherm and Thermodynamic Approaches. *Results in Surfaces and Interfaces*, *16*, 100281. https://doi.org/10.1016/j.rsurfi.2024.100281

[24] Li, S., Huang, L., Guo, W., Feng, X., Cao, Y., & Liao, B. (2024). Two-Dimensional Copper-Based Metal-Organic Framework for Efficient Removal of Methylene Blue from Wastewater. *European Journal of Inorganic Chemistry*, *27*(26), e202400240. https://doi.org/10.1002/ejic.202400240

[25] Khan, M. A., ALOthman, Z. A., Naushad, M., Khan, M. R., & Luqman, M. (2015). Adsorption of Methylene Blue on Strongly Basic Anion Exchange Resin (Zerolit DMF): Kinetic, Isotherm, and Thermodynamic Studies. *Desalination and Water Treatment*, *53*(2), 515-523. https://doi.org/10.1080/19443994.2013.838527

[26] Farooq, N., Shanableh, A., Qureshi, A. M., Jabeen, S., & Rehman, A. (2022). Synthesis and Characterization of Clay Graphene Oxide Iron Oxide (Clay/GO/Fe_2O_3)-Nanocomposite for Adsorptive Removal of Methylene Blue Dye from Wastewater. *Inorganic Chemistry Communications*, *145*, 109956. https://doi.org/10.1016/j.inoche.2022.109956

[27] Turna, T., Solmaz, A., & Baran, A. (2025). Rapid Adsorption of Methylene Blue by Synthesizing Zinc Oxide Nanoparticles from *Ocimum basilicum* L. Waste. *International Journal of Environmental Science and Technology*, *22*, 10049-10066. https://doi.org/10.1007/s13762-025-06492-4

[28] Satyam, S., & Patra, S. (2024). Innovations and Challenges in Adsorption-Based Wastewater Remediation: A Comprehensive Review. *Heliyon*, *10*(9), e29573. https://doi.org/10.1016/j.heliyon.2024.e29573

[29] Fouda-Mbanga, B. G., Onotu, O. P., & Tywabi-Ngeva, Z. (2024). Advantages of the Reuse of Spent Adsorbents and Potential Applications in Environmental Remediation: A Review. *Green Analytical Chemistry*, *11*, 100156. https://doi.org/10.1016/j.greeac.2024.100156

[30] Akhtar, M. S., Ali, S., & Zaman, W. (2024). Innovative

Adsorbents for Pollutant Removal: Exploring the Latest Research and Applications. *Molecules*, *29*(18), 4317. https://doi.org/10.3390/molecules29184317

[31] Wang, Y., Yang, P., Zheng, L., Shi, X., & Zheng, H. (2020). Carbon Nanomaterials with sp^2 or/and *sp* Hybridization in Energy Conversion and Storage Applications: A Review. *Energy Storage Materials*, *26*, 349-370. https://doi.org/10.1016/j.ensm.2019.11.006

[32] Lim, S. Y., Shen, W., & Gao, Z. (2015). Carbon Quantum Dots and Their Applications. *Chemical Society Reviews*, *44*(1), 362-381. https://doi.org/10.1039/C4CS00269E

[33] Wu, M., Zhan, J., Geng, B., He, P., Wu, K., Wang, L., Xu, G., Li, Z., Yin, L., & Pan, D. (2017). Scalable Synthesis of Organic-Soluble Carbon Quantum Dots: Superior Optical Properties in Solvents, Solids, and LEDs. *Nanoscale*, *9*(35), 13195-13202. https://doi.org/10.1039/C7NR04718E

[34] Ukanwa, K. S., Patchigolla, K., Sakrabani, R., Anthony, E., & Mandavgane, S. (2019). A Review of Chemicals to Produce Activated Carbon from Agricultural Waste Biomass. *Sustainability*, *11*(22), 6204. https://doi.org/10.3390/su11226204

[35] Yavari, Z., & Noroozifar, M. (2017). Kinetic, Isotherm and Thermodynamic Studies with Linear and Non-Linear Fitting for Cadmium(II) Removal by Black Carbon of Pine Cone. *Water Science and Technology*, *76*(8), 2242-2253. https://doi.org/10.2166/wst.2017.375

[36] Pundlik, R. C., Chowdhury, S. D., Dash, R. R., & Bhunia, P. (2021). Life-cycle assessment of agricultural waste-based and biomass-based adsorbents. In A. Pandey, R. Dayal Tyagi & S. Varjani (Eds), *Biomass, Biofuels, Biochemicals* (pp. 669-695). Elsevier Inc. https://doi.org/10.1016/B978-0-12-821878-5.00004-0

[37] Akhtar, F., Andersson, L., Ogunwumi, S., Hedin, N., & Bergström, L. (2014). Structuring Adsorbents and Catalysts by Processing of Porous Powders. *Journal of the European Ceramic Society*, *34*(7), 1643-1666. https://doi.org/10.1016/j.jeurceramsoc.2014.01.008

[38] Baur, G. B., Yuranov, I., & Kiwi-Minsker, L. (2015). Activated Carbon Fibers Modified by Metal Oxide as Effective Structured Adsorbents for Acetaldehyde. *Catalysis Today*, *249*, 252-258. https://doi.org/10.1016/j.cattod.2014.11.021

[39] Peng, X., Luan, Z., Di, Z., Zhang, Z., & Zhu, C. (2005). Carbon Nanotubes-Iron Oxides Magnetic Composites as Adsorbent for Removal of Pb (II) and Cu (II) from Water. *Carbon*, *43*(4), 880-883. https://doi.org/10.1016/j.carbon.2004.11.009

[40] Hu, J., Song, Z., Chen, L., Yang, H., Li, J., & Richards, R. (2010). Adsorption Properties of MgO(111) Nanoplates for the Dye Pollutants from Wastewater. *Journal of Chemical & Engineering Data*, *55*(9), 3742-3748. https://doi.org/10.1021/je100274e

[41] Khan, M. M., Khan, W., Ahamed, M., & Alhazaa, A. N. (2017). Microstructural Properties and Enhanced Photocatalytic Performance of Zn Doped CeO_2 Nanocrystals. *Scientific Reports*, *7*, 12560. https://doi.org/10.1038/s41598-017-11074-7

[42] Hassanzadeh-Tabrizi, S. A., Motlagh, M. M., & Salahshour, S. (2016). Synthesis of ZnO/CuO Nanocomposite Immobilized on γ-Al_2O_3 and Application for Removal of Methyl Orange. *Applied Surface Science*, *384*, 237-243. https://doi.org/10.1016/j.apsusc.2016.04.165

[43] Koohestanian, E., Samimi, A., Mohebbi-Kalhori, D., & Sadeghi, J. (2017). Sensitivity Analysis and Multi-Objective Optimization of CO_2CPU Process Using Response Surface Methodology. *Energy*, *122*, 570-578. https://doi.org/10.1016/j.energy.2017.01.129

[44] Mehta, A., Mishra, A., Basu, S., Shetti, N. P., Reddy, K. R., Saleh, T. A., & Aminabhavi, T. M. (2019). Band Gap Tuning and Surface Modification of Carbon Dots for Sustainable Environmental Remediation and Photocatalytic Hydrogen Production - A Review. *Journal of Environmental Management*, *250*, 109486. https://doi.org/10.1016/j.jenvman.2019.109486

[45] Gomroki, S., Yavari, Z., Abbasian, A. R., Afarani, M. S., & Noroozifar, M. (2022). Stabilizing Nano-Pd on Porous Li_2TiO_3 via Chemical and Electrochemical Reduction Systems for the Electrooxidation of Ethylene Glycol. *Materials Chemistry and Physics*, *281*, 125896. https://doi.org/10.1016/j.matchemphys.2022.125896

[46] Hosseini, S. A., Abbasian, A. R., Gholipoor, O., Ranjan, S., & Dasgupta, N. (2019). Adsorptive Removal of Arsenic from Real Sample of Polluted Water Using Magnetic GO/$ZnFe_2O_4$ Nanocomposite and $ZnFe_2O_4$ Nanospinel. *International Journal of Environmental Science and Technology*, *16*, 7455-7466. https://doi.org/10.1007/s13762-018-2140-x

[47] Nakamoto, K. (2008). *Infrared and Raman Spectra of Inorganic and Coordination Compounds, Part B: Applications in Coordination, Organometallic, and Bioinorganic Chemistry*. John Wiley & Sons. https://doi.org/10.1002/9780470405888

[48] Mahalingam, T., Selvakumar, C., Kumar, E. R., & Venkatachalam, T. (2017). Structural, Optical, Morphological and Thermal Properties of TiO_2-Al and TiO_2-Al_2O_3 Composite Powders by Ball Milling. *Physics Letters A*, *381*(21), 1815-1819.

https://doi.org/10.1016/j.physleta.2017.02.053

[49] Emam, A. N., Loutfy, S. A., Mostafa, A. A., Awad, H., & Mohamed, M. B. (2017). Cyto-Toxicity, Biocompatibility and Cellular Response of Carbon Dots–Plasmonic Based Nano-Hybrids for Bioimaging. *RSC Advances*, *7*(38), 23502-23514. https://doi.org/10.1039/C7RA01423F

[50] Gao, Y., Li, Y., Zhang, L., Huang, H., Hu, J., Shah, S. M., & Su, X. (2012). Adsorption and Removal of Tetracycline Antibiotics from Aqueous Solution by Graphene Oxide. *Journal of Colloid and Interface Science*, *368*(1), 540-546. https://doi.org/10.1016/j.jcis.2011.11.015

[51] Chao, Y., Zhu, W., Wu, X., Hou, F., Xun, S., Wu, P., Ji, H., Xu, H., & Li, H. (2014). Application of Graphene-Like Layered Molybdenum Disulfide and Its Excellent Adsorption Behavior for Doxycycline Antibiotic. *Chemical Engineering Journal*, *243*, 60-67. https://doi.org/10.1016/j.cej.2013.12.048

[52] Foo, K. Y., & Hameed, B. H. (2010). Insights into the Modeling of Adsorption Isotherm Systems. *Chemical Engineering Journal*, *156*(1), 2-10. https://doi.org/10.1016/j.cej.2009.09.013

[53] Akhtar, M., Sarfraz, M., Ahmad, M., Raza, N., & Zhang, L. (2025). Use of Low-Cost Adsorbent for Waste Water Treatment: Recent Progress, New Trend and Future Perspectives. *Desalination and Water Treatment*, *321*, 100914. https://doi.org/10.1016/j.dwt.2024.100914

[54] López-Luna, J., Ramírez-Montes, L. E., Martinez-Vargas, S., Martínez, A. I., Mijangos-Ricardez, O. F., González-Chávez, M. D., Carrillo-González, R., Solís-Domínguez, F. A., Cuevas-Díaz, M. D., & Vázquez-Hipólito, V. (2019). Linear and Nonlinear Kinetic and Isotherm Adsorption Models for Arsenic Removal by Manganese Ferrite Nanoparticles. *SN Applied Sciences*, *1*(8), 950. https://doi.org/10.1007/s42452-019-0977-3

[55] Mercado-Borrayo, B. M., Schouwenaars, R., Litter, M. I., Montoya-Bautista, C. V., & Ramírez-Zamora, R. M. (2014). Metallurgical slag as an efficient and economical adsorbent of arsenic. In S. Ahuja (Ed.), *Water Reclamation and Sustainability* (pp. 95-114). Elsevier. https://doi.org/10.1016/B978-0-12-411645-0.00005-5

[56] Batzias, F. A., & Sidiras, D. K. (2004). Dye Adsorption by Calcium Chloride Treated Beech Sawdust in Batch and Fixed-Bed Systems. *Journal of Hazardous Materials*, *114*(1-3), 167-174. https://doi.org/10.1016/j.jhazmat.2004.08.014

[57] Khattri, S. D., & Singh, M. K. (2000). Colour Removal from Synthetic Dye Wastewater Using a Bioadsorbent. *Water, Air, and Soil Pollution*, *120*(3), 283-294. https://doi.org/10.1023/A:1005207803041

[58] Tsai, W. T., Hsu, H. C., Su, T. Y., Lin, K. Y., & Lin, C. M. (2008). Removal of Basic Dye (Methylene Blue) from Wastewaters Utilizing Beer Brewery Waste. *Journal of Hazardous Materials*, *154*(1-3), 73-78. https://doi.org/10.1016/j.jhazmat.2007.09.107

[59] Ozdemir, F. A., Demirata, B., & Apak, R. (2009). Adsorptive Removal of Methylene Blue from Simulated Dyeing Wastewater with Melamine-Formaldehyde-Urea Resin. *Journal of Applied Polymer Science*, *112*(6), 3442-3448. https://doi.org/10.1002/app.29835

[60] Kavitha, D., & Namasivayam, C. (2007). Experimental and Kinetic Studies on Methylene Blue Adsorption by Coir Pith Carbon. *Bioresource Technology*, *98*(1), 14-21. https://doi.org/10.1016/j.biortech.2005.12.008

[61] Srihari, V., & Das, A. (2008). The Kinetic and Thermodynamic Studies of Phenol-Sorption onto Three Agro-Based Carbons. *Desalination*, *225*(1-3), 220-234. https://doi.org/10.1016/j.desal.2007.07.008

[62] Jamal, R., Zhang, L., Wang, M., Zhao, Q., & Abdiryim, T. (2016). Synthesis of Poly(3,4-propylenedioxy-thiophene)/MnO_2 Composites and Their Applications in the Adsorptive Removal of Methylene Blue. *Progress in Natural Science: Materials International*, *26*(1), 32-40. https://doi.org/10.1016/j.pnsc.2016.01.001

[63] Peighambardoust, S. J., Rezaei-Aghdam, S., Niroumand, J. S., Pakdel, P. M., & Sillanpää, M. (2025). Efficient Methylene Blue Elimination from Water Media by Nanocomposite Adsorbent-Based Carboxymethyl Cellulose-Grafted Poly(acrylamide)/ Magnetic Biochar Decorated with ZIF-67. *RSC Advances*, *15*(39), 32407-32423. https://doi.org/10.1039/D5RA03796D

Additional information

Correspondence and requests for materials should be addressed to Z. Yavari.

HOW TO CITE THIS ARTICLE

Bazzi, M.; Yavari, Z.; Shahbakhsh, M. (2025). Adsorption of methylene blue on lithium titanate and its composite with carbon dots: Optimization of parameters and adsorbent recovery, *J. Part. Sci. Technol. 11 (1) 101-116.*

DOI: 10.22104/jpst.2026.8046.1288
URL: https://jpst.irost.ir/article_1687.html